Development and Kinematic Analysis of a Redundant, Modular and Backdrivable Laparoscopic Surgery Robot

Alaa Alassi, Nural Yilmaz, Merve Bazman, Berke Gur and Ugur Tumerdem

***Abstract*— In this paper, we propose a novel redundant robotic forceps system with a modular architecture. We also provide a kinematic solution for the control of the proposed system as well as similar redundant and modular systems. Robots used in laparoscopic surgery usually require 6-7 axes for the positioning of the tool tips of laparoscopic surgery instruments within the patient body. These are cartesian x, y, z, roll, pitch, yaw and grasping axes. The cartesian positioning is achieved by an external Remote Center of Motion (RCM or RCoM) mechanism that can control the position of the instrument tip with a spherical motion at the incision-trocar entry point. While tip cartesian positions are controlled by the external mechanism, the intra-corporeal bending motions are achieved by 3-4 DOF wrist mechanisms which are usually articulated to the RCM mechanisms in macro-micro form. In this paper, we propose a kinematic control method for achieving RCM motion with general 6-7 axis robot arms, as well as a macro-micro architecture that utilizes such 6 axis robot arms and 3-4 DOF wrist mechanisms. Here, we use a novel back-drivable wrist mechanism that can achieve 90 degree pitch, yaw, and gripping motions. The obtained design and equations are also validated with experiments on a prototype that we have built. Experiment results show that an operator unilaterally controls the motion of the forceps, through a haptic interface, as desired.**

I. INTRODUCTION

The introduction of robotics in minimally invasive surgery (MIS) has led to substantial improvements in the way which these operations are carried out. Among these improvements are higher accuracy, precision, and dexterity as well as tremor filtering [1][2]. In addition, robotic MIS systems reduce cognitive and physical effort on the part of the surgeon by automatically handling the mapping required to mirror the motion of the laparoscopic tool inside the patient.

An important milestone in robotic MIS was reached in the year 2000 when the da Vinci Surgical System by Intuitive surgical received the FDA approval [3]. Since then, Da Vinci has become the primary robotic system for general purpose laparoscopic surgery [4]. However, da Vinci still lacks the capability of haptic rendering and feedback of tool-tissue interaction forces, which is vital for effectively performing the surgery. Force feedback in real-time renders the mechanical properties of the tissue at a master command interface, providing virtual constraints on the surgeons motion that improves the quality of surgical tool telemanipulation [5]. Only recently, two haptically enhanced surgical robots became available to the market, namely the Senhance System and REVO-I [4]. The former is a commercial version of TELELAP AlF-X [6] approved by the FDA [7]. The TELELAP AlF-X was also granted the CE mark for the European market [4]. The latter system is approved by the Korean FDA only and, therefore is currently restricted to the Korean market [4]. Unfortunately, technical details about the kinematic design, system architecture, and haptic rendering degrees-of-freedom (DOF) are not published for either system. Hence, the design of robotic platforms with haptic capabilities for MIS remains a matter of active research and development. To this end, different robotic MIS systems are being developed. Kim *et. al.* [8] developed a compact 7-DOF robotic platform (namely, S-Surge) that is comprised of a 3-DOF hybrid remote center of motion (RCM) mechanism integrated with a 4-DOF surgical instrument. Although S-Surge supports 6-DOF motion with one additional grasping DOF, the kinematic analysis provided for the system does not include the combined manipulator/instrument system and is limited to the 3-DOF RCM mechanism. Furthermore, force feedback is limited to the 3 manipulating and one grasping DOF. The RAVEN system is a surgical robotic platform that provides 6 motion DOF and an additional grasping DOF. The design of RAVEN was kinematically optimized based on a database of spatial and dynamic measurements [9]. However, RAVEN is also a mainly cable driven mechanism which introduces back-drivability issues manifested in controller, as well as contact force estimation problems due to the nonlinear characteristic of the cables [10].

The first and foremost objective of this paper is to introduce a new robotic MIS system design that addresses the above discussed shortcomings of existing robotic MIS systems. The proposed surgical robotic platform provides:

- 6-DOF surgical tool motion,
- 6-axis force/torque feedback,
- back-drivability,
- modularity.

The proposed architecture integrates the compliant commercial 7-DOF KUKA LBRV IIWA manipulator with an in-house designed 3-DOF parallel wrist mechanism. Since

A. Alassi is with the Department of Mechatronics Engineering, Bahcesehir University, Besiktas, Istanbul, 34353, Turkey
(email: alaa.alassi1@stu.bahcesehir.edu.tr)

N. Yilmaz is with the Department of Mechanical Engineering, Marmara University, Goztepe, Kadikoy, Istanbul, 34722, Turkey
(email: nural.yilmaz@marun.edu.tr)

M. Bazman is with the Department of Mechanical Engineering, Marmara University, Goztepe, Kadikoy, Istanbul, 34722, Turkey
(email: mervebazman@marun.edu.tr)

B. Gur is with the Department of Mechatronics Engineering, Bahcesehir University, Besiktas, Istanbul, 34353, Turkey
(email: berke.gur@eng.bau.edu.tr)

U. Tumerdem is with the Department of Mechanical Engineering, Marmara University, Goztepe, Kadikoy, Istanbul, 34722, Turkey
(email: ugur.tumerdem@marmara.edu.tr)

this integration results in a hyper-redundant system with complex kinematics, the second objective of this paper is to introduce a kinematic analysis method termed the Virtual Laparoscopic Robotic Instrument through which the surgical instrument motion is decoupled from the kinematics of the driving mechanism. This decoupling simplifies the inverse kinematics and singular configuration solutions of the surgical tool without dealing with the complexities of the driving manipulator.

This paper is organized as follows: overview of the system and integration architecture is described in Section II, Section III explains the kinematic analysis, Section IV presents experiment results, and the conclusion is provided by Section V.

II. System Overview

A. The 3-DOF Parallel Wrist Mechanism

To do the intra-corporeal bending and gripping motions, 4-DOF robotic forceps mechanism that is a combination of a gripper and 3-DOF dexterous and parallel wrist mechanism which consists of 3-RSR serial chain in the wrist and 3-PRR serial chain in the actuation part was designed. A gripper can easily be integrated to the top platform of the wrist but this paper omits the gripper in experiments, as it is not critical in the kinematic solution.

The 3-DOF parallel wrist mechanism is actuated with 3 linear motors and rigid rods as can be seen in Figure 1. This wrist mechanism can perform 2-DOF rotation (pitch and yaw) and radial translation (thrust) motions. It has the capability of 90-degree rotations in pitch and yaw axes. Also, it can pass through narrow incisions by changing its effective radius through its thrust motion. Furthermore, this wrist mechanism provides high back-drivability in all axes since rigid rods are used in the system for transmission. This means that a force applied at the end-effector of the wrist can be transmitted directly to the motors and be estimated. The design details and the kinematic solution of the wrist mechanism were presented in [11].

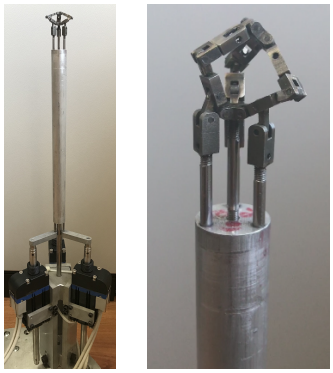

(a) (b)

Fig. 1. The manufactured 3-DOF wrist mechanism prototype (a) Whole mechanism (b) Wrist part

Fig. 2. The 7 degrees of freedom robotic manipulator Kuka LBR IIWA 7 R800.

B. The Kuka IIWA 7 R800 Robot

To provide RCM, the anthropomorphic robotic manipulator Kuka LBR IIWA is used (Figure 2). IIWA can be actuated in impedance mode in joint or task space, which makes the robot back drivable and safe for robot human interactions. Another remarkable aspect is that the robot supports real-time position, force and torque control. Also IIWA is easily integrable to other systems through the Fast Robot Interface (FRI) which is a UDP based real-time bi-directional interface for sending commands to actuators and getting state feedback from the sensors [12][13]. Moreover, the manipulator is equipped with highly sensitive torque sensors which eliminate the need for additional force sensors. Finally, due to its kinematics, its possible to move the elbow in what is called a self-motion manifold. Such motion can be utilized to increase the dexterity or workspace [14] in addition to providing the possibility of moving the elbow away in case a human intervention is needed and the robot is hindering the human motion during the surgery.

C. Integration Architecture

The developed wrist mechanism and the commercial Kuka IIWA robot can be integrated as depicted in Figure 3. The architecture is based on multiprocessing and networking. Multiprocessing is handled by the first host computer (H-1) which is running two major processes:

- The interface to IIWA controller (FRI client). This process handles the communication with IIWA controller.
- A UDP based client node. This process handles the communication between the haptic device (Omega6) and H-1 in one side, and the communication between H-1 and the second host computer (H-2) on the other side.

These two processes exchange data through a shared memory segment, allocated by the operating system. Hence, other processes such as (a process handling and processing a camera stream) can be integrated into the system through accessing the shared memory segment. As such integrability is guaranteed. After Omega6 commands and IIWA state are acquired, they are sent through the UDP client node to the server node hosted by H-2. The server node is

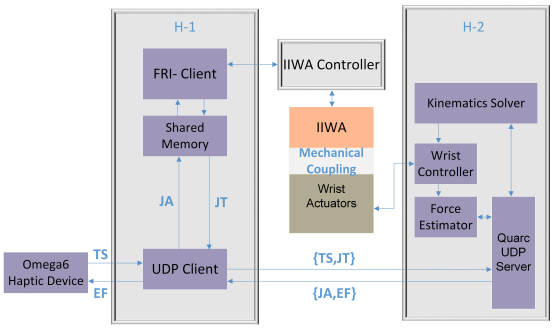

Fig. 3. A functional diagram representing the distributed control scheme of the proposed surgical robotic platform. Where JA and JT are IIWA's Joint angles and torques respectively, TS is task space command, and EF is the estimated forces and torques at the wrist tool.

running on Quarc [15] which is a real-time operating system that uses Windows to execute controller routine. Also, this node is responsible for: computing the inverse kinematics, controlling the wrist, as well as running the external force estimator.

III. Kinematic Analysis

A. Virtual Laparoscopic Robotic Instrument

The motion in manual laparoscopic surgeries is composed of three motion types:

1) A pivoting motion about the insertion point known as The remote center of motion(RCM).
2) Insertion.
3) Roll motion

1 and 2 can be modeled with virtual joints: two revolute and a prismatic joint (RRP) with mutually orthogonal axes intersecting at the insertion point. This structure provides translational motion with a spherical workspace that has a radius equal to the insertion depth provided by the prismatic joint. By adding a fourth revolute joint to represent the roll motion, the motion model of manual laparoscopy (also referred to as (4DOF RCM [16]) is fully covered by (RRPR) robotic structure as illustrated in Figure 4. Since this structure is inadequate to perform six degrees of freedom motion, a wrist mechanism with two orthogonal revolute joints can be integrated at the end of the insertion rod. This will result in a 'virtual' 6-DOF robot with (RRPRRR) structure. As such, given the desired wrist transformation, (RRR) orients the wrist whereas, (RRP) positions the insertion link accordingly. Thus, by defining a base frame centered at the trocar (Figure 5), a kinematic model of this virtual robot can be obtained using the Denavit-Hartenberg convention. As a result, forward, inverse and velocity kinematics can be obtained using the traditional formulations.

In this study, the degrees of freedom that are responsible for the manual laparoscopic motion (RRPR) are referred to as ψ, ϕ , ρ and γ, respectively. The motion of these virtual joints is provided by the robotic manipulator IIWA after performing the necessary mapping. While α and β are real joints, their motion is provided by the integrated robotic wrist. Figure 5 depicts the concept of the proposed Virtual Laparoscopic Robotic Instrument model.

TABLE I
DH parameters of the Virtual Laparoscopic Robotic Instrument

Joint	a_{i-1}	α_{i-1}	d_i	θ_i
1	0	$-\pi/2$	0	$-\pi/2+\phi$
2	0	$-\pi/2$	0	$-\pi/2+\psi$
3	0	$-\pi/2$	0	0
4	0	0	ρ	γ
5	0	$\pi/2$	0	$\pi/2+\alpha$
6	0	$\pi/2$	0	$\pi/2+\beta$

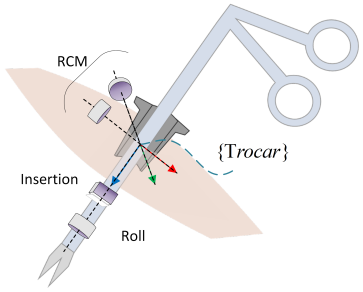

Fig. 4. RRPR Model of the manual laprascopic motion.

B. Forward Kinematics

It is essential to perform forward kinematic analysis to obtain symbolic representations of link transformations that will later be used to obtain the inverse kinematics. Frame assignment Figure 5 and the DH parameters in table I are obtained using the modified convention. Also, link transformations are obtained through:

$$ {}^{i-1}_{i}\mathbf{T} = \begin{bmatrix} \mathrm{c}\theta_i & -\mathrm{s}\theta_i & 0 & a_{i-1} \\ \mathrm{s}\theta_i\mathrm{c}\alpha_{i-1} & \mathrm{c}\theta_i\mathrm{c}\alpha_{i-1} & -\mathrm{s}\alpha_{i-1} & -\mathrm{s}\alpha_{i-1}d_i \\ \mathrm{s}\theta_i\mathrm{s}\alpha_{i-1} & \mathrm{c}\theta_i\mathrm{s}\alpha_{i-1} & \mathrm{c}\alpha_{i-1} & \mathrm{c}\alpha_{i-1}d_i \\ 0 & 0 & 0 & 1 \end{bmatrix} \quad (1) $$

C. Inverse Kinematics

${}^{0}_{G}T$ is the reference transformation matrix in Eq.2 which defines the target position and orientation.

$$ {}^{0}_{G}T = \left[\begin{array}{ccc|c} & R_G & & P_G \\ \hline 0 & 0 & 0 & 1 \end{array}\right] \quad (2) $$

The first step is to find $\vec{\rho}$ that represents the insertion depth in a vector form, from Figure 7 it is obvious that:

$$ \vec{\rho} = \vec{P}_G - \vec{d} \quad (3) $$

P_G is the desired position that is the last column of the desired transformation matrix ${}^{0}_{G}T$ excluding the homogeneous part. And, $\vec{d}$ is obtained from:

$$ \vec{d} = -dY_6 \quad (4) $$

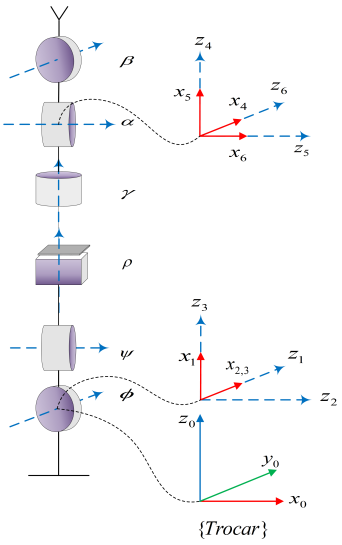

Fig. 5. Frame assignment of the Virtual Laparoscopic Robotic Instrument using the modified convention.Trocar is equivalent to frame 0

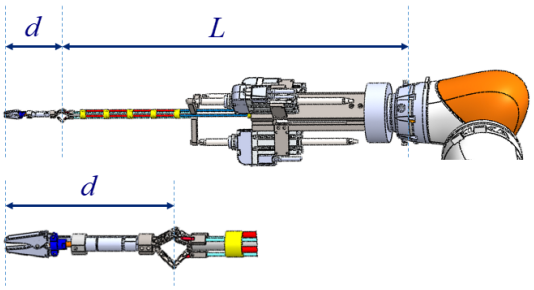

Fig. 6. Visualizing forceps dimensions.

where d is the distance between wrist center and tip of the gripper which is a summation of thrust distance and gripper length (refer to Figure 6) . And, Y_6 is,

$$Y_6 = R_G \begin{bmatrix} 0 \\ 1 \\ 0 \end{bmatrix} \tag{5}$$

Since $\vec{\rho}$ is described with respect to $\{0\}$, ϕ can be calculated by using the components of $\vec{\rho}$ on frame $\{0\}$ as visualized in Figure 7,

$$\phi = \text{atan2}({}^0\rho_x, {}^0\rho_z) \tag{6}$$

To calculate ψ, from Figure 7 we realize that ψ is equal to the angle between $\vec{\rho}$ and x_1 as they are two angles with mutually perpendicular sides. This angle can be obtained by plunging ϕ value into Eq.1 and ${}^0_1T$ can be computed. Then $\vec{\rho}$ is described in the first frame by premultiplying by the inverse of ${}^0_1T$,

$${}^1\vec{\rho} = ({}^1_0T){}^0\vec{\rho} \tag{7}$$

Thus ψ is obtained utilizing $\vec{\rho}$ components on frame $\{1\}$,

$$\psi = \text{atan2}(-{}^1\rho_z, {}^1\rho_x) \tag{8}$$

The remaining angles of the RRR structure α, β, and γ can

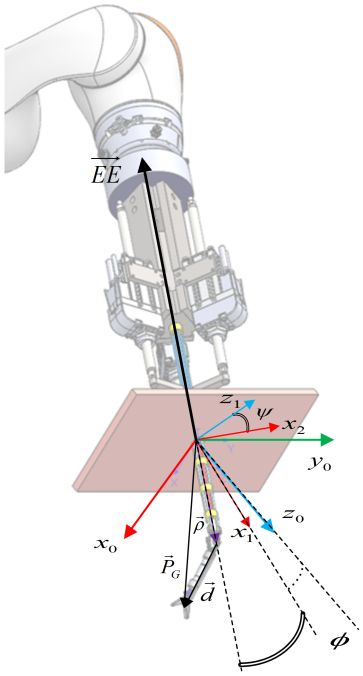

Fig. 7. Visualization of the RCM joints ϕ,ψ and ρ in addition to $\vec{P_G}$ and $\vec{d}$ vectors.

be obtained algebraically by noticing that:

$${}^3\mathbf{R}_G = ({}^0_3\mathbf{R}^{-1})\mathbf{R}_G \tag{9}$$

Since ϕ and ψ are available, ${}^0_3\mathbf{R}$ can be computed using forward kinematics. On the other hand, ${}^0_3\mathbf{R}$ can also be obtain symbolically using forward kinematics as well. The result is:

$${}^3_6\mathbf{R} = \begin{bmatrix} c_\beta s_\gamma + c_\gamma s_\alpha s_\beta & c_\gamma c_\beta s_\alpha - s_\gamma s_\beta & c_\gamma c_\alpha \\ s_\gamma s_\alpha s_\beta - c_\gamma c_\beta & c_\beta s_\gamma s_\alpha + c_\gamma s_\beta & c_\alpha s_\gamma \\ -c_\alpha s_\beta & -c_\alpha c_\beta & s_\alpha \end{bmatrix} \tag{10}$$

Considering the numeric values of ${}^3_6\mathbf{R}$ to be r_{ij}, the solution yields to:

$$\alpha = \text{asin}(r_{33}) \tag{11}$$

$$\beta = \text{atan2}(-r_{31}, -r_{32}) \tag{12}$$

$$\gamma = \text{atan2}(r_{23}, r_{13}) \tag{13}$$

where $-90^o < \beta < 90^o$, $-175^o \leq \gamma \leq 175^o$ and $-90^o < \alpha < 90^o$.

Notice that for systems that use a prismatic joint to feed the insertion (*i.e.*, da Vinci) [18], ρ can directly be provided by that prismatic joint's motion. Whereas for systems that use the Cartesian motion of the end effector to drive the insertion (*i.e.*, DLR MIRO) [19] and the system presented in this paper, further computations are necessary. In order to map ${}^0\vec{\rho}$ to the end effector position ${}^0\overrightarrow{EE}$, the unit vector of ${}^0\vec{\rho}$ can first be defined in the form of

$$\vec{u} = \frac{{}^0\vec{\rho}}{\|{}^0\vec{\rho}\|} \tag{14}$$

Since ${}^0\vec{\rho}$ and ${}^0\overrightarrow{EE}$ are collinear, and noticing that their directions are opposite, ${}^0\overrightarrow{EE}$ can be calculated with the following formula:

$$ {}^0\overrightarrow{EE} = -(L-\rho)\vec{u} \tag{15}$$

where L is the total length between the end effector the wrist center Figure 6. Also, notice that for any driving mechanism, maintaining the RCM constrain requires the orientation of the end effector to have the same orientation of frame $\{4\}$, thus:

$$ {}^0_{EE}\mathbf{R} = {}^0_4\mathbf{R} \tag{16}$$

D. Jacobian and Singularity Analysis

The Jacobian is a matrix that maps joint space to task space velocities. This mapping is expressed in the form of [17]:

$$ \dot{\mathcal{V}} = \mathbf{J}\dot{q} \tag{17}$$

where $\dot{\mathcal{V}}$ is a vector of task space velocities expressed in the Jacobian frame, and $\dot{q}$ is the joint space velocity vector. Using equation 17 the velocity of the wrist tool frame described in the trocar frame can be obtained. A symbolic form of the Jacobian can be obtained using Robotica package provided by [20] with taking into account necessary modifications to comply with the modified convention. Eq. 18 shows Jacobian matrix of the Virtual Laparoscopic Robotic Instrument where the notations of c and s symbolize $cosine$ and $sine$ functions, respectively.

Singularities can be obtained as well when the determinant of the Jacobian is zero :

$$ Det(\mathbf{J}) = -\rho^2 \mathrm{c}_\psi \mathrm{c}_\alpha \tag{19}$$

Thus, 19 is zero when

$$\begin{aligned} \rho &= 0 \\ \psi &= \pm\pi/2 \\ \alpha &= \pm\pi/2 \end{aligned} \tag{20}$$

These singularities agree with inverse kinematics solution. Indeed, as α approaches 90 degrees, γ and β changes instantaneously form $\pi/2$ to $-\pi/2$ or vise versa, since the denominator of equations 12 and 13 contains $cos\alpha$. The same discussion is valid for ψ, when the denominator of equation 6 is zero. The most serious case happens when ρ is near zero, small motion of the wrist tool requires a very large motion for the driving manipulator. Also, notice, when $\rho = 0$ the robot loses two operational space degrees of freedom, since moving the insertion rod on x and y will no longer be possible.

Recognizing these singularities is significant for systems that use artificially constrained RCM because the controller might fail to maintain the constraint.

IV. Experiments

A. Validation of Rotational Motion

The objective of this experiment is to assess the performance of the system when executing pure rotational commands: pitch, yaw, and roll. Since the translational commands are fixed, consequently, the system must maintain the commanded position while the orientation is changing. Using the haptic device, the operator commands the angular trajectory while the translational trajectory is fixed at (0,0,135) mm on x,y, and z, respectively w.r.t trocar. The executed joint space trajectory is recorded for 71.9 sec with 1 kHz sampling frequency and used to reproduce the link transformations which are used to reproduce the posture of the virtual robot. In this experiment the system was computing the inverse kinematics considering a gripping tool is mounted on top of the wrist, but because the tool was not available at the time of the experiment, the tool motion is represented by its posture as illustrated in Figure 8. To quantify the ability of the system in maintaining the commanded position, the mean and standard deviation of the executed position trajectory are calculated. Ideally, the mean should be equal to the commanded position, that happens when the system succeeds to keep all trajectory samples at a commanded position, therefore, bias from the mean represents a systematic error. This error is caused by the accuracy of the encoders as well as the steady-state error of both IIWA and the wrist controllers. The results presented in Table II indicates a good accuracy of less than 0.2 mm. On the other hand, the small standard deviation indicates an acceptable precision with less than 2 mm. This random error is mostly due to differences in the dynamic response for two robots causing asynchronous motion between ψ, ϕ, γ, and ρ in one side and α and β in the other.

TABLE II

Statistical values of the orientation experiment. The values are measured in mm.

$Value$	x	y	z
μ	-0.1227	-0.1886	135.1938
σ	1.4577	1.7878	0.4581

B. Validation of Translational Motion

Another experiment was also performed to validate the inverse kinematics of the system. The task is to touch a predetermined set of pins inside a phantom patient (Figure 9) in a zigzag path to mimic stitching motion. The motion of the operators hand is captured by the haptic device and the robot follows the trajectory created by the master. During the telemanipulation, the position of the wrist tool is computed using forward kinematics (gripper length is taken as 0, since the experiment setup does not include a gripper). The commanded and the executed trajectories recorded in real-time with a sampling frequency of 1 KHz. The results are illustrated in Figure 10. Because our phantom setup is for conventional laparoscopy, and the camera and display angle is not ideal as in the case of da Vinci system, it can be a little difficult for the operator to control the robot, however the experiment shows that the operator can successfully control the position of the tool.

$$J = \begin{pmatrix} \rho c_\phi c_\psi & -\rho s_\phi s_\psi & c_\psi s_\phi & 0 & 0 & 0 \\ 0 & -\rho c_\psi c_\phi{}^2 - \rho c_\psi s_\phi{}^2 & -s_\psi & 0 & 0 & 0 \\ -\rho c_\psi s_\phi & -\rho c_\phi s_\psi & c_\phi c_\psi & 0 & 0 & 0 \\ 0 & c_\phi & 0 & c_\psi s_\phi & c_\phi c_\gamma + s_\phi s_\psi s_\gamma & c_\gamma c_\alpha s_\phi s_\psi - c_\phi c_\alpha s_\gamma + c_\psi s_\phi s_\alpha \\ 1 & 0 & 0 & -s_\psi & c_\psi s_\gamma & c_\psi c_\gamma c_\alpha - s_\psi s_\alpha \\ 0 & -s_\phi & 0 & c_\phi c_\psi & c_\phi s_\psi s_\gamma - c_\gamma s_\phi & c_\alpha s_\phi s_\gamma + c_\phi \left(c_\gamma c_\alpha s_\psi + c_\psi s_\alpha\right) \end{pmatrix} \tag{18}$$

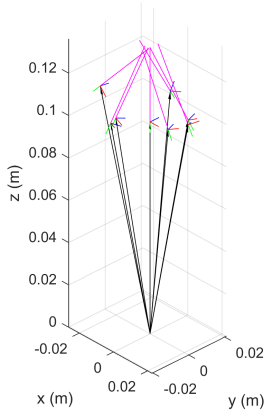

Fig. 8. Posture plot of the Virtual Laparoscopic Robotic Instrument for randomly selected samples of the executed trajectory showing the wrist tool (magenta) and its frame while approaching a target point from different directions. The insertion link (black) performing RCM motion to compensate for the translational motion of the wrist tool to maintain the fixed commanded position.

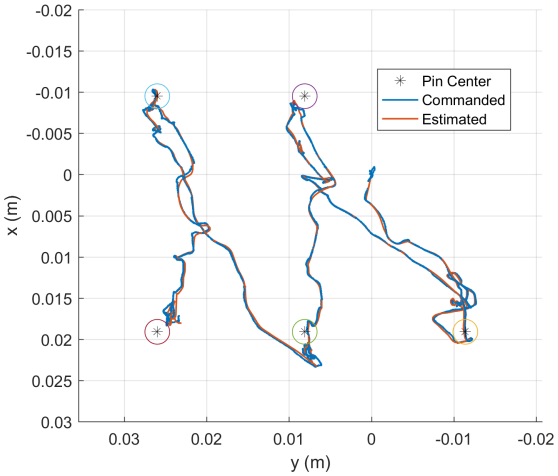

Fig. 10. A comparison between the commanded and the executed path.The circle around each targeted pin represents the circumference of the targeted pin.

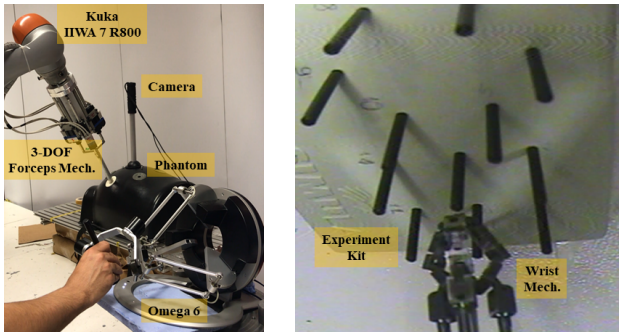

(a) (b)

Fig. 9. Experiment setup of the surgical robot (a) Utilized devices (b) Inside the phantom

V. CONCLUSION

This paper proposes a novel redundant forceps system with a modular architecture and a kinematic solution for the control of the proposed and similar redundant and modular systems. Kinematic position analysis is performed by using the proposed Virtual Laparoscopic Robotic Instrument Method. Furthermore, the Jacobian matrix is obtained to identify the singularities of the 6 DOF laparoscopic motion. Finally, experiments were conducted on a phantom patient. The experiments demonstrated that the proposed robotic forceps platform can track the human hand motions obtained from a haptic interface in real time, as desired. The experiment results also validate the efficacy of the presented design and validity of the kinematic analysis. In the future, force estimation and bilateral teleoperation will be implemented on the proposed system. Also different gripper mechanisms will be integrated to the current platform.

VI. ACKNOWLEDGMENT

This research was supported by The Scientific and Technological Research Council of Turkey (TUBITAK) project 115E712.

REFERENCES

[1] V. Vitiello, S. L. Lee, T. P. Cundy, and G. Z. Yang, "Emerging Robotic Platforms for Minimally Invasive Surgery", In IEEE Reviews in Biomedical Engineering, vol. 6, pp. 111-126, 2013.
[2] S. Kalan, S. Chauhan, R.F. Coelho, M. A. Orvieto, I. R. Camacho, K.J. Palmer, and V.R. Patel, "History of Robotic Surgery", Journal of Robotic Surgery (2010), 4(3), 141-147.
[3] http://www.roboticoncology.com/history-of-robotic-surgery/
[4] P.P. Rao, "Robotic surgery: new robots and finally some real competition!", World Journal of Urology (2018): 1-5.
[5] C. R. Wagner, N. Stylopoulos, P. G. Jackson, and R. D. Howe, The benefit of force feedback in surgery: Examination of blunt dissection,Presence , vol. 16, no. 3, pp. 252262, 2007.
[6] S. Gidaro, M. Buscarini, E. Ruiz, M. Stark, and A. Labruzzo, "Telelap Alf-X: a novel telesurgical system for the 21st century", Surgical Technology International 22 (2012): 20-25.
[7] https://www.fda.gov/NewsEvents/Newsroom/PressAnnouncements /ucm580452.htm

[8] U. Kim, D.H. Lee, Y. B. Kim, D. Y. Seok, J. So, and H. R. Choi, "S-Surge: Novel Portable Surgical Robot with Multiaxis Force-Sensing Capability for Minimally Invasive Surgery", IEEE/ASME Transactions on Mechatronics, vol. 22, no. 4 (2017): 1717-1727.

[9] M. J. H. Lum, D. C. W. Friedman, G. Sankaranarayanan, H. King, K. Fodero, R. Leuschke, B. Hannaford, J. Rosen, and M. N. Sinanan, "The RAVEN: Design and Validation of a Telesurgery System", The International Journal of Robotics Research 28, no. 9 (2009): 1183-1197.

[10] S. N. Kosari, S. Ramadurai, H. J. Chizeck, and B. Hannaford, "Control and Tension Estimation of a Cable Driven Mechanism Under Different Tensions", In ASME 2013 International Design Engineering Technical Conferences and Computers and Information in Engineering Conference, pp. V06AT07A077-V06AT07A077. American Society of Mechanical Engineers, 2013.

[11] M.Bazman, N. Yilmaz, U. Tumerdem, "Dexterous and Back-Drivable Parallel Robotic Forceps Wrist for Robotic Surgery", In IEEE conference on Advanced Motion Control, AMC 2018, Tokyo, Japan, March 2018

[12] "Kuka sunrise.connectivity fri 1.5 v3 manual", KUKA Roboter GmbH.

[13] G. Schreiber, A. Stemmer, and R. Bischoff, "The Fast Research Interface for the KUKA Lightweight Robot", In IEEE Workshop on Innovative Robot Control Architectures for Demanding (Research) Applications How to Modify and Enhance Commercial Controllers (ICRA 2010) (pp. 15-21). Citeseer,2010. p. 15-21.

[14] I. Kuhlemann, A. Schweikard, P. Jauer, and F. Ernst, "Robust inverse kinematics by configuration control for redundant manipulators with seven DOF", 2016 2nd International Conference on Control, Automation and Robotics (ICCAR), Hong Kong, 2016, pp. 49-55. doi: 10.1109/ICCAR.2016.7486697

[15] https://www.quanser.com/

[16] C. H. Kuo, and J.S. Dai, "Kinematics of a Fully-Decoupled Remote Center-of-Motion Parallel Manipulator for Minimally Invasive Surgery", Journal of Medical Devices, 6(2), p.021008.,May 07, 2012.

[17] J. J. Craig (2005), "Introduction to Robotics: Mechanics and Control", (Pearson: Upper Saddle River, NJ) p. 135-164.

[18] G. A. Fontanelli, F. Ficuciello, L. Villani, B. Siciliano, "Modelling and Identification of the da Vinci Research Kit Robotic Arms", In 2017 IEEE/RSJ International Conference on Intelligent Robots and Systems 2017.

[19] U. Hagn, M. Nickl, S. Jrg , G. Passig, T. Bahls, A. Nothhelfer, F. Hacker, L. Le-Tien, A. Albu-Schffer, R. Konietschke, M. Grebenstein, R. Warpup, R. Haslinger, M. Frommberger, and G. Hirzinger, "The DLR MIRO: a versatile lightweight robot for surgical applications", Industrial Robot: An International Journal. 2008 Jun 20;35(4):324-36.

[20] J. F. Nethery, M. W. Spong, "Robotica: a Mathematica package for robot analysis", In IEEE Robotics & Automation Magazine, vol. 1, no. 1, pp. 13-20, March 1994.